Assessing Age Related Cranial Characteristics and Morphometrics of the Egyptian Rousette (Rousettus aegyptiacus) from Central Africa

Authors: Nkoana, Tlaishego T., Kearney, Teresa, and Markotter, Wanda

Source: Acta Chiropterologica, 25(1) : 169-181

Published By: Museum and Institute of Zoology, Polish Academy of Sciences

URL: https://doi.org/10.3161/15081109ACC2023.25.1.010

Acta Chiropterologica, 25(1): 169–181, 2023
PL ISSN 1508-1109 © Museum and Institute of Zoology PAS
doi: 10.3161/15081109ACC2023.25.1.010

Assessing age related cranial characteristics and morphometrics of the Egyptian rousette (*Rousettus aegyptiacus*) from Central Africa

TLAISHEGO T. NKOANA[1, 2], TERESA KEARNEY[2, 3, 4], and WANDA MARKOTTER[1]

[1]*Department of Medical Virology, Centre for Viral Zoonoses, University of Pretoria, Bophelo Road, Prinshof 349-Jr, Pretoria, 0084, South Africa*
[2]*Department of Zoology and Entomology, University of Pretoria, Lynnwood Road, Hatfield, Pretoria, 0002, South Africa*
[3]*Ditsong National Museum of Natural History, 432 Paul Kruger Street, Pretoria Central, Pretoria, 0001, South Africa*
[4]*Corresponding author: E-mail: kearney@ditsong.org.za*

This study assessed and related quantitative age determination methods based on cranial bone fusion and dental development to linear morphometrics in *Rousettus aegyptiacus*. Five growth development stages were identified based on cranial suture fusion and degree of second molar tooth eruption. Expressing these growth development stages in measurement size showed a linear growth pattern, with little overlap between smaller (stages 1, 2, and 3) and larger (stages 4 and 5) individuals. Total skull length (TSL), mastoid breadth (MB) and forearm length (FAL) had the highest influence on variation along the first and second principal components, accounting for 93% of variation. Advanced size was confirmed to relate to aging owing to development of cranial suture fusions and dental development. The smallest and largest individuals were significantly ($P < 0.05$) separated by measurements of TSL, MB and FAL. Meanwhile, some intermediate sized individuals overlapped despite being in different stages of cranial suture development. Species specific reliability in morphological approaches to age determination can be achieved by establishing a baseline reference, which may be directly related to the quantitative cementum growth assessment method.

Key words: age, growth, postnatal, morphometrics, development, *Rousettus aegyptiacus*

INTRODUCTION

Bats, order Chiroptera, possess a uniquely long-lived lifespan with some species reaching up to 30 years of age (Wilkinson and South, 2002; Monadjem *et al.*, 2020). A hypothesis for longevity in bats is the reduction in metabolic rate during torpor and hibernation has an inverse relationship to lifespan as toxic accumulation of metabolic by-products is decreased in bats (Brunet-Rossinni and Wilkinson, 2009). However, non-hibernating bats also display longevity (Wilkinson and South, 2002). This relatively long lifespan makes bats unique subjects for postnatal growth development studies, which follows a similar pattern of events as other organisms (Brunet-Rossinni and Austad, 2004; Oli and Coulson, 2016). These events include juvenile development, sexual maturity, first reproduction, senescence and death (Brunet-Rossinni and Wilkinson, 2009; Eghbali *et al.*, 2018). Information derived from postnatal growth development research can be used to understand characteristics associated with age such as growth rates, longevity, timing of sexual maturity and reproduction (Eghbali *et al.*, 2018).

Few studies have been conducted on the postnatal growth patterns of bats with approximately 5% of the over 1,400 species being reported (Brunet-Rossinni and Austad, 2004). These bats belong to the families Hipposideridae — *Hipposideros terasensis* (Cheng and Lee, 2002) and *Hipposideros cineraceus* (Jin *et al.*, 2010); Phyllostomidae — *Phyllostomus hastatus* (Stern and Kunz, 1998) and *Artibeus watsoni* (Chaverri and Kunz, 2006); Pteropodidae — *Rousettus leschenaulti* (Elangovan *et al.*, 2002), *Cynopterus sphinx* (Elangovan *et al.*, 2003), *Pteropus poliocephalus* (Divljan *et al.*, 2006; Welbergen, 2010), *Pteropus* sp. (Giannini *et al.*, 2006), and *Eidolon helvum* (Hayman *et al.*, 2012*b*); Molossidae — *Tadarida brasiliensis* (Allen *et al.*, 2010); Thyropteridae — *Thyroptera tricolor* (Chaverri and Vonhof, 2011); Vespertilionidae — *Myotis lucifugus* (Baptista *et al.*, 2000), *Eptesicus fuscus* (Hood *et al.*, 2002), *Pipistrellus pipistrellus* (Hielscher *et al.*, 2015), *Scotophilus kuhlii* (Chen *et al.*, 2016), *Myotis*

emarginatus (Eghbali and Sharifi, 2018), and *Chalinolobus gouldii* (Eastick *et al.,* 2022). All these studies assessed morphological and quantifiable characteristics which can be tracked ordinally throughout the lifespan of a bat using methods that examined dental degradation, body mass growth, sexual maturity, fusion of the epiphysis, cranial bone fusion, tooth development and skeletal growth (Baptista *et al.*, 2000; Cheng and Lee, 2002; Divljan *et al.*, 2006; Giannini *et al.*, 2006; Brunet-Rossinni and Wilkinson, 2009; Hielscher *et al.*, 2015). Except for Divljan *et al.* (2006) and Hayman *et al.* (2012*b*), these studies used rapid, non-destructive methods that do not harm live animals or damage preserved specimens which enabled examination of either infant bats of known age (Stern and Kunz, 1998; Baptista *et al.*, 2000; Cheng and Lee, 2002; Elangovan *et al.*, 2002, 2003; Chaverri and Kunz, 2006; Allen *et al.*, 2010; Chaverri and Vonhof, 2011; Eghbali and Sharifi, 2018; Eastick *et al.*, 2022) or preserved specimens of unknown age (Giannini *et al.*, 2006; Hielscher *et al.*, 2015).

Of interest are cranial bone fusion, tooth development and skeletal growth. Cranial bone fusion development was used by Giannini *et al.* (2006) to describe and arrange *Pteropus* sp. individuals into different stages of development ranging from pup to adults. In addition to cranial bone fusion, Giannini *et al.* (2006) relied on qualitative factors including degree of tooth eruption, tooth wear, and tooth loss to place individuals into respective developmental stages. In a quantitative assessment of the insectivorous species *Noctilio leporinus*, Monrroy *et al.* (2019) relied on variations in degree of suture fusion to separate growth development into juvenile, subadult and adult stages.

Skeletal growth development has been used in some postnatal growth studies to determine age (Baptista *et al.*, 2000; Cheng and Lee, 2002; Elangovan *et al.*, 2002; Brunet-Rossinni and Wilkinson, 2009). Using linear morphometrics, these have primarily focused on age determination in juvenile bats of less than a year old and have commonly used a regression equation to determine age in younger juveniles, using forearm length, and older juveniles, using epiphyseal gap (Baptista *et al.*, 2000; Cheng and Lee, 2002; Elangovan *et al.*, 2002). Age determining regression equations are species specific and limited to younger bats (Brunet-Rossinni and Wilkinson, 2009). For older sub-adults and adults, age determination using linear morphometrics has been given less attention, albeit linear morphometrics has been used as a tool to describe species (Shahbaz *et al.*, 2014) or show variations between sexes and species (Storz *et al.*, 2001; Taylor and Monadjem, 2008; Jarrín-V. *et al.*, 2010).

The widespread *Rousettus aegyptiacus* (E. Geoffroy St.-Hilaire, 1810), commonly called the Egyptian rousette, is of focus to the present study. Though previous assessments were undertaken for this species (Noll, 1979), information on growth development characteristics for this species remains inadequate despite implications in disease and conservation research (Hyatt *et al.*, 2004; Keeling and Rohani, 2008; Brunet-Rossinni and Wilkinson, 2009; Hayman *et al.*, 2012*a*). Several potentially zoonotic viruses have been identified in *R. aegyptiacus* including Henipa related paramyxoviruses, Sosuga virus, Marburg virus and the rabies related lyssavirus Lagos bat virus (Hyatt *et al.*, 2004; Lloyd-Smith *et al.*, 2005; Swanepoel *et al.*, 2007; Keeling and Rohani, 2008; Hayman *et al.*, 2012*a*; Pawęska *et al.*, 2018; Markotter *et al.*, 2020). Age and sex influence viral prevalence and has been well documented in human and veterinary medicine that investigated their influence on virus infection outcome and shedding, and carrier status development (Hyatt *et al.*, 2004; Keeling and Rohani, 2008; Amman *et al.*, 2012; Hayman *et al.*, 2012*a*; Hayman, 2015). Conservation strategies rely on studies on age and sex determination as factors that contribute towards self-sufficiency, disease susceptibility, socialization, and exposure to predation (Hecht, 2021).

This study assessed age and sex variation in *R. aegyptiacus* from Central Africa, by using and comparing non-destructive methods, which evaluated morphological development associated with aging. We aimed to (1) categorise specimens into various stages of postnatal growth development based on cranial bone fusion elements and molar tooth eruption, and (2) assess the alignment of these stages to linear cranial measurements. We hypothesized that growth development stages derived from cranial bone fusion and molar tooth eruption assessment can be predicted by cranial linear morphometrics.

Materials and Methods

Preserved dry skulls of *R. aegyptiacus* from the Ditsong National Museum of Natural History (DNMNH), South Africa were used in lieu of sampling new specimens. These specimens were originally collected from Goroumbwa Mine (3.108895, 29.578227), Durba, Democratic Republic of Congo (DRC) in May and October 1999 as part of a study which investigated an outbreak of Marburg haemorrhagic fever and associated

reservoir hosts including *R. aegyptiacus* (see Swanepoel *et al.*, 2007). Ethical approval (NAS304/2021) from the University of Pretoria Animal Ethics Committee was obtained.

Skulls (n = 153, see Supplementary Table S1) were measured using Mitutoyo callipers (Kawasaki, Kanagawa, Japan) with a 0.01 mm accuracy. Most of the measurements were from the skull, with one long bone measurement, taken by Swanepoel *et al.* (2007), included. Measurements of skull length and width were used by Shahbaz *et al.* (2014) on *Rousettus leschenaulti* including greatest skull length, breadth of braincase and mandibular tooth row length. However, Shahbaz *et al.* (2014) lacked in-depth statistical analysis that compared morphological variations between specimens. Storz *et al.* (2001) provided a multivariate analysis to describe variation between sexes of the Pteropodid *Cynopterus sphinx* using limb measurements. References for statistically in-depth studies on skull-based intraspecific and interspecific variations in the size and sexual dimorphism of bats was found for the much smaller sized Vespetilionid *Murina* spp. (Schmieder *et al.*, 2015; Son *et al.*, 2015). Similar to Shahbaz *et al.* (2014), Schmieder *et al.* (2015) and Son *et al.* (2015) included length and breadth measurements, but also included height. Following Shahbaz *et al.* (2014), Schmieder *et al.* (2015) and Son *et al.* (2015), cranial and dentary measurements that captured two-dimensional size were measured (Fig. 1): total skull length (TSL), rostral length (RL), rostral width (RW), braincase width (BW), mastoid breadth (MB) and dental length (DENL). Forearm length (FAL), a long bone measurement commonly used in age determination studies of bats (Brunet-Rossinni and Wilkinson, 2009), and easily measured in the field, was measured by the collector (see Swanepoel *et al.*, 2007) and was also included. Except for specimens with a damaged mandible, mastoid, occipital condyle or rostrum, all specimens from Durba, regardless of size, were measured.

The cranial bone fusion of each specimen (n = 153) was also examined under a Carl Zeiss STEMI 2000 W-PI 10x/23 light microscope with a KL 200 stereomicroscope light source (Carl-Zeiss-Straße 22, 73447 Oberkochen, Germany). We focused on the fusion/partial fusion/non-fusion of the most conspicuous sutures of the different regions of the skull to group specimens in an ordinal manner from youngest (lesser number of fused sutures) to oldest (greatest number of fused sutures), following cranial suture terminology reported by Giannini *et al.* (2006) and Monrroy *et al.* (2019). Sutures of the basicranial region (synchondrosis sphenoccipitali-sspo), occipital region (sutura parietointerparietalis-spip, sutura occipitointerparietalis-soipa, and sutura occipitoparietalis-sopa), and vault region (sutura coronalis-sc, sutura sagittalis-ss) were used (Fig. 2). The presence/absence and shape of the crista sagittalis (cs) were also included in grouping *R. aegyptiacus* into different development stage groups (Fig. 2). Younger Ptreropodids, as reported by Giannini *et al.* (2006), were observed to have deciduous incisors, canines and premolar and a permanent first molar. These were later replaced by permanent teeth and the eruption of the second molar. Tooth eruption of the second molar (M2) along the medial and labial cusps was therefore considered where no eruption, partial eruption, or full eruption can be observed (Fig. 2).

A principal component analysis (PCA) (STATS package, version 4.0.3, 2020) was conducted to assess and visualize cranial and dentary size variation in multivariate space. The

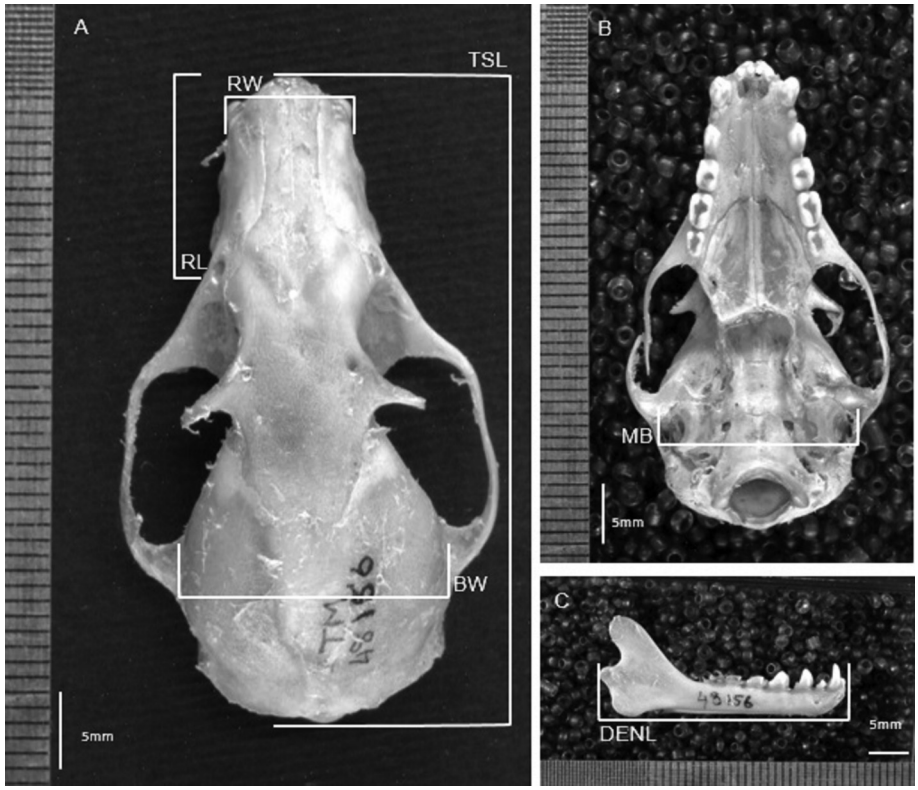

FIG. 1. Dorsal (A) and ventral (B) skull, and lateral mandible (C) views illustrating the measurements: total skull length (TSL), rostral width (RW), rostral length (RL), braincase width (BW), mastoid breadth (MB) and dental length (DENL). Scale = 0.5 mm and 1 mm gradations

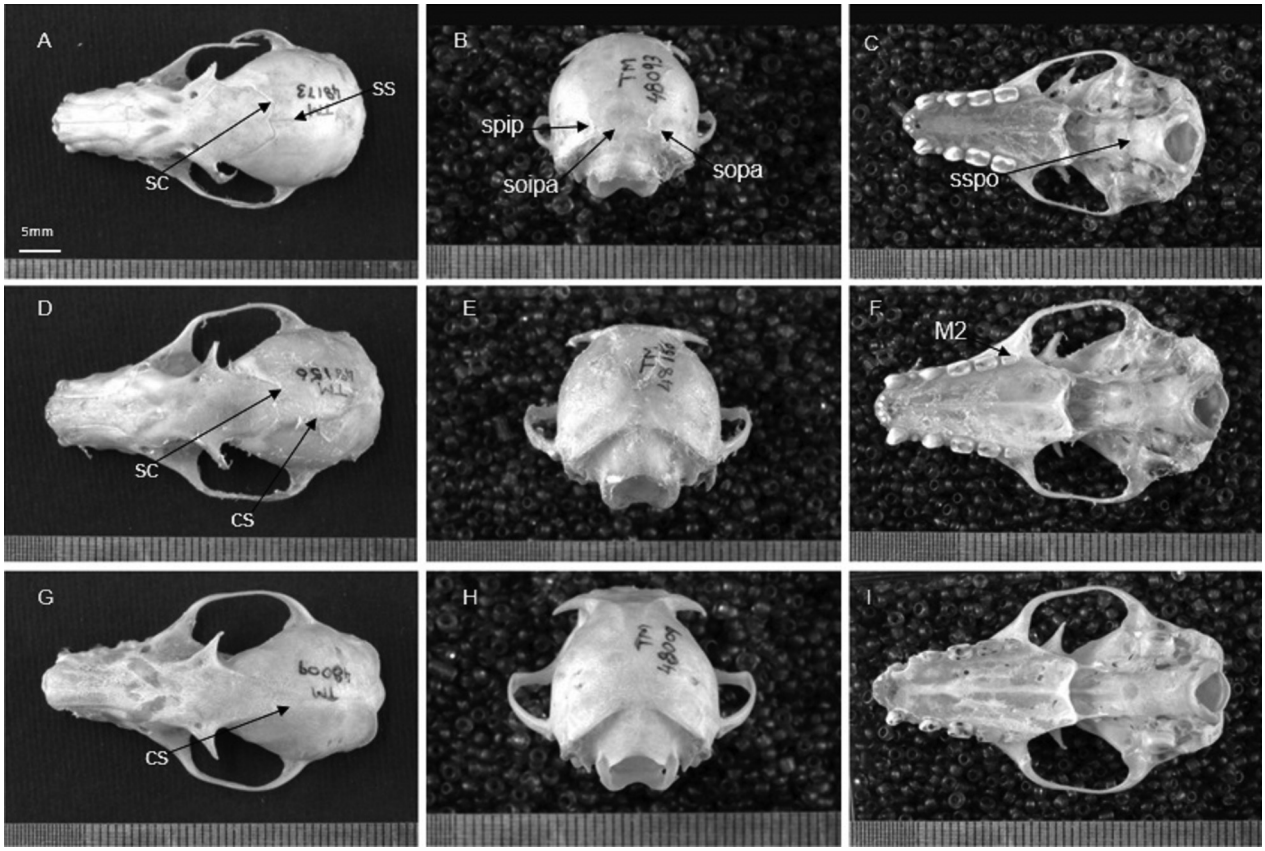

FIG. 2. Dorsal, posterior and ventral views of *R. aegyptiacus* skulls at different stages of cranial and molar eruption development. The ascending development suture fusion and second molar eruption is shown for specimens in (A, B, C) younger less developed stages, (D, E, F) a penultimate stage, and an (G, H and I) older advanced stage. Abbreviations: synchondrosis sphenoccipitali (sspo), sutura parietointerparietalis (spip), sutura occipitointerparietalis (soipa), sutura occipitoparietalis (sopa), sutura coronalis (sc), sutura sagittalis (ss), crista sagittalis (cs), and second molar (M2). Scale = 0.5 mm and 1 mm gradations

correlation and quartiles of the measurements with the highest and lowest PCA loadings along first and second PC's were visualized using XY scatter plots (Rcmdr package, version 2.7.1, 2020) and violin plots (ggplot2 package, version 3.3.5, 2021), respectively. The mean, standard deviation (SD), minimum and maximum were determined for all seven measurements (n = 153; ♀♀ n = 62 and ♂♂ n = 91). All the variables (measurements) had a non-normal distribution ($P < 0.01$, Shapiro-Wilk normality test), therefore non-parametric statistical tests were employed. Outliers were identified by multiplying the interquartile range (IQR) by 1.5 and 3 for slight and strong outliers respectively (Schwertman *et al.*, 2004). A Wilcoxon rank sum test was used to evaluate sexual dimorphism, whilst variation between development stage groups was tested using a Kruskal-Wallis H (KW-H) test. Any significant variation found using the KW-H was further tested using a post-hoc Dunn test to identify variations at individual level. We used linear discriminant function analysis (DFA) to test the accuracy of assigning specimens of a given measurement into cranial suture/tooth eruption based development stage groups. Since a DFA requires datasets with equal variances, we used Levene's test for homogeneity of variance (centred on the mean) to test for equal variances and excluded variables with unequal variances. All statistics were conducted on RStudio (Version 1.4.1103, 2021) using the statistical coding language R (version 4.0.3, 2020; R Core Team, 2021).

RESULTS

Quantitative assessment of the development of second molar, six cranial sutures and the sagittal crest in female and male *R. aegyptiacus* specimens (n =153) yielded five growth development stages (Table 1). Less developed stages were interpreted as having a lesser number of fused sutures whilst more developed stages displayed a greater number of fused sutures. In the assessment, three degrees of sutures fusion were observed and recorded as unfused, partially fused (anteriorly or posteriorly) or fused. Suture fusion was similar for the younger stages 1, 2 and 3 where sc and sspo were unfused, whilst ss was either unfused or partially fused and all three degrees of fusion were observed for spip. The soipa and sopa were either fused or unfused for these stages (Table 1). The degree of suture fusion varied in stages 1 to 3 in terms of ss (unfused, posteriorly fused, fused), spip (unfused, anteriorly fused, fused), soipa (unfused, fused) and sopa (unfused, fused). The penultimate stage 4 skull surface had

TABLE 1. Stages of development based on tooth eruption of the second molar and fusion of cranial elements as observed in *R. aegyptiacus* collected from Goroumbwa Mine, Durba, DRC. Cranial elements include molar two (M2) eruption, the sutures: synchondrosis sphenoccipitali (sspo), sutura coronalis (sc), sutura sagittalis (ss), sutura parietointerparietalis (spip), sutura occipitointerparietalis (soipa), sutura occipitoparietalis (sopa), and the crista sagittalis (cs). Bold fonts indicate new change in development from previous stage

Trait	Stage 1	Stage 2	Stage 3	Stage 4	Stage 5
M2 eruption	No eruption	**Partial eruption**	**Full eruption**	Full eruption	Full eruption
Sspo	Unfused	Unfused	Unfused	**Fused**	Fused
Sc	Unfused	Unfused	Unfused	Unfused	**Fused**
Ss	Unfused/posteriorly fused	Unfused/posteriorly fused	Unfused/posteriorly fused	**Unfused/posteriorly fused/fused**	Fused
Spip	Unfused/anteriorly fused/fused	Unfused/anteriorly fused/fused	Unfused/anteriorly fused/fused	**Anteriorly fused/fused**	**Fused**
Soipa	Unfused/fused	Unfused/fused	Unfused/fused	Unfused/fused	Fused
Sopa	Unfused/fused	Unfused/fused	Unfused/fused	**Fused**	Fused
Cs	Absent	Absent	**Absent/early development**	**Absent/early development/present**	**Present**

fused sspo and sopa, unfused sc, and either unfused, posteriorly fused or fused ss (Table 1).

The crista sagittalis (cs) was present in some stages 3 and 4 specimens at an early development stage where the labial lines were conspicuous. In stage 5, the sspo, sc, ss, spip, soipa and sopa were all fully fused (Table 1). The development of the sagittal ridge (cs) was absent in stages 1 and 2. Early development of the cs was observed in stage 3 where two lateral ridges adjacent to the frontal of the skull had formed. In stage 4, the cs was absent, in early development or present whilst the cs was fully developed in stage 5. An ascending growth pattern characterized less advanced dental and suture development in stages 1 and 2, succeeded by fully erupted M2 molars in stage 3 and subsequent advanced development in stages 4 and 5, was presented.

A PCA plot showed this ascending growth pattern in multivariate space after aligning morphological measurements (BW, DENL, FAL, MB, RL, RW and TSL) to growth development stages (Fig. 3). Two outlier females (TM48233, TM48229) with negative scores across the *x*-axis were found to significantly differ ($P < 0.05$) from other stage 5 males (Fig. 3). Further inspection revealed that TM48233 and TM48229 had relatively smaller rostral widths that are two SDs lower than the mean of other stage 5 specimens. In addition, both specimens had relatively minute infraorbital foramen. Further variation between sexes was observed for the larger specimens where TSL greater than 44 mm was only measured in the males. Although both analysed and observed variations were not regarded as sexual dimorphism, it prompted separate analyses of females and males.

The first principal component (PC1), which was interpreted as linear size, explained 89% of variation for both sexes. Factor loadings along PC1 were positive for all the variables with TSL and MB having the most influence on variation by scoring the highest and lowest loadings, respectively (Table 2). Female and male specimens assigned to stages 4 and 5 primarily overlapped on the positive side of PC1, which associated them to overall greater linear size for the tested variables TSL, BW, DENL, FAL, MB, RL, RW. In contrast, female and male specimens in stages 1, 2 and 3 overlapped on the negative side of PC1 associating them to smaller linear size for all the tested variables. Furthermore, specimens assigned to stages 1, 2 and 3 significantly differed ($P < 0.05$) to specimens in stages 4 and 5. Meanwhile, PC2 accounted for 4% of variation which was primarily influenced by MB and FAL that had the

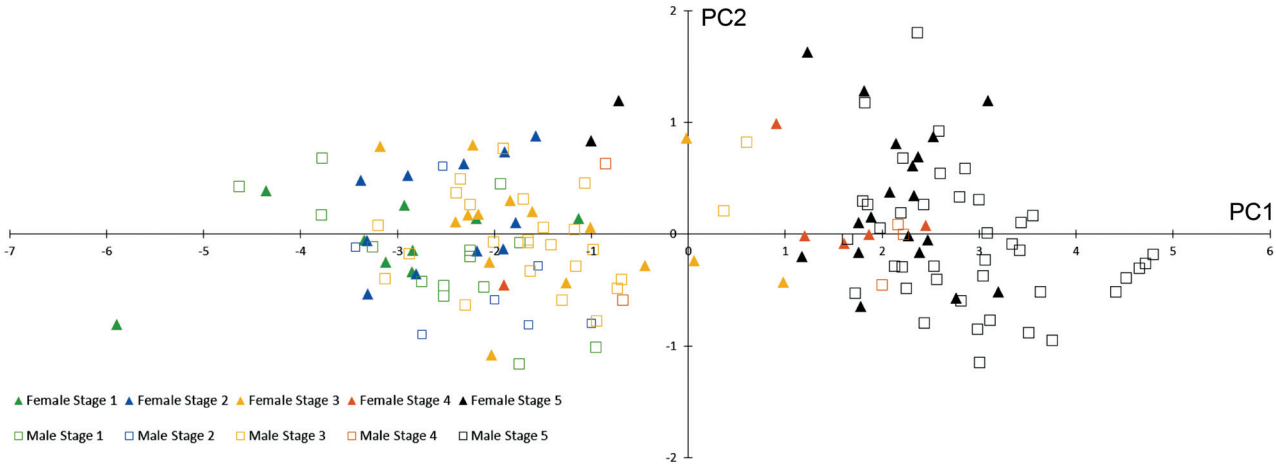

FIG. 3. Principal component (PC) plot for PC1 and PC2 scores of linear measurements taken from *R. aegyptiacus* specimens (n = 153) collected in the Democratic Republic of the Congo (DRC). Specimens are separated by growth stages 1 (green), 2 (blue), 3 (yellow), 4 (orange), 5 (black). The females are represented by opaque triangles whilst males are empty square. PC1 explained 89% of linear size variation for both sexes along the positive (II and III) and negative (I and IV) quadrants. PC2 explained 4% of variation along the positive (I and II) and negative (III and IV) quadrants

highest and lowest factor loadings, respectively. No significant variation ($P > 0.05$) was found between the scores on the second principal component (PC2). The forearm length (FAL), one cranial width (RW), and all cranial length (DENL, RL, TSL) measurements had positive factor loadings along PC2 (Table 2). The other cranial width measurements (BW and MB) had negative loadings.

Further analysis of the alignment of linear measurement to growth development stages focused on TSL, MB and FAL given the influence of these variables on linear size variation. The median, lower and upper quartiles of smaller males in stages 1, 2 and 3 overlapped for TSL, MB and FAL (Fig. 4). For females, a similar overlap for these measurements was seen except for TSL in stage 3 specimens where all three quartiles were higher than stages 1 and 2 with no overlap (Fig. 4). Differences in TSL, MB and FAL were not significant ($P > 0.05$) between stages 1, 2 and 3 (for combined data), within the same sex, and between sexes. Except for the two aforementioned stage 5 females (TM48233 and TM48229), differences in measurements were not significant $P > 0.1$) between stages 4 and 5, within the same sex, and between sexes. The medians, lower and upper quartiles of stage 4 and 5 females overlapped for TSL, MB and FAL whilst, for males, quartiles were higher and non-overlapping for the three measurements (Fig. 4). Strict significant ($P < 0.05$) values separated the smaller specimens (stages 1, 2 and 3) from the larger (stages 4 and 5) specimens for TSL, MB and FAL. This is further depicted by a higher density of specimens in stages 4 and 5 compared to stages 1, 2 and 3 (Fig. 4).

For TSL, specimens (female and male) of stages 1–3 which measured less than 36.0 mm were significantly ($P < 0.05$) smaller than their respective stage 4–5 counterparts that measured above 42.0 mm. Furthermore, the MB of specimens in stages 1–3 (< 14.8 mm for females and < 14.9 mm for males) were significantly ($P < 0.05$) smaller than stages 4–5 specimens that measured above 16.0 mm. For FAL, stage 4–5 specimens (female and male) that measured greater than 97.0 mm were significantly larger ($P < 0.05$) than stage 1–3 specimens less than 85.0 mm although two stage 4 specimens (TM48083 and TM48223) also measured below 85.0 mm. These two stage 4 specimens, together with TM48002, were further found to have posteriorly fused sagittal sutures (Table 1). Both female

TABLE 2. PC loadings for morphological measurements of *R. aegyptiacus* (n = 153). Standard deviation (SD) and proportion of variance for PC1, PC2 and PC3 which account for 96% of variation are shown. Abbreviations: TSL — total skull length, RL — rostral length, RW — rostral width, BW — braincase width, MB — mastoid breadth, DENL — dental length, FAL — forearm length

Variable	PC1	PC2	PC3
TSL	0.393*	0.176	0.209
RL	0.387	0.270	-0.140
RW	0.371	0.105	-0.736*
BW	0.370	-0.425	-0.383
MB	0.355*	-0.745*	0.354*
DENL	0.388	0.252	0.351
FAL	0.382	0.292*	0.119
SD	2.490	0.560	0.430
Variance (%)	0.890	0.040	0.030

* — Variables with the lowest and highest factor loadings

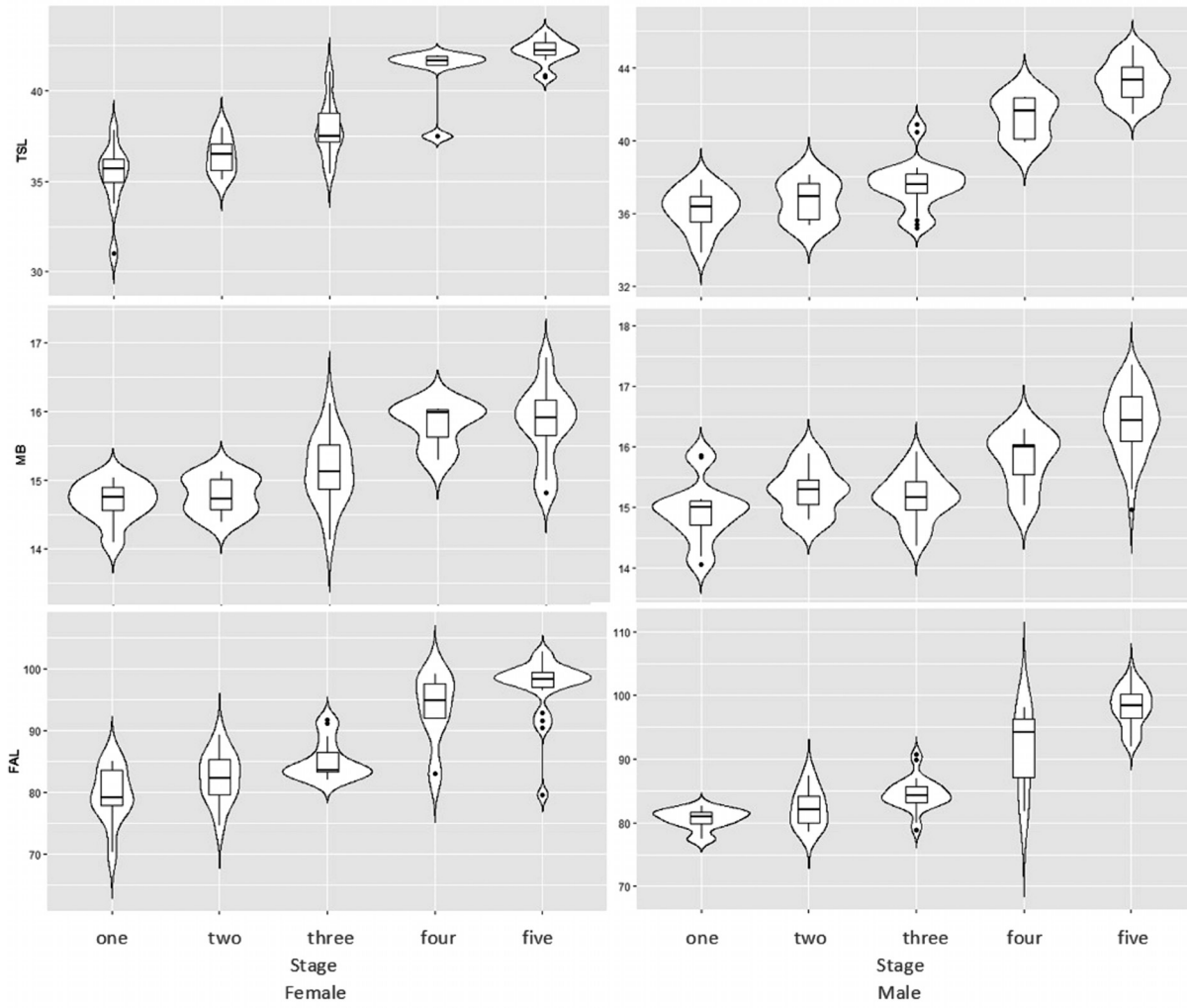

FIG. 4. Violin plots depicting the boxplots (minimum, 1st quartile, median, 3rd quartile and maximum) and density of female (n = 62) and male (n = 91) specimens for total skull length (TSL), mastoid breadth (MB) and forearm length (FAL)

and male specimens that measured between the above values (i.e. 14.8 mm < MB < 16.0 mm; 36.0 mm < TSL < 42 mm; and 85.0 mm < FAL < 97 mm) did not differ significantly ($P > 0.1$) in relation to the different stage groups. This is further depicted in Fig. 4 where the specimens in the lower and upper quartiles, and maximums of the smaller stages 1–3 overlap with the minimums and lower quartile of the larger stages 4–5.

A linear growth pattern was observed when plotting TSL versus MB and FAL versus MB (Fig. 5) where strong, positive correlation was found between TSL vs MB (r_s = 0.83, $P < 0.01$), and FAL vs MB (r_s = 0.76, $P < 0.01$). Both plots reiterated the PCA plot (Fig. 3) where growth ascended from smaller (stages 1, 2 and 3) to larger (stages 4 and 5) specimens (Fig. 5). As growth increased, the least squares line of the males got slightly higher than the females in both plots (Fig. 5A and 5B). As depicted in the PCA plot (Fig. 3), the measurements TSL, MB and FAL expressed a linear progression of growth, with a fair amount of scatter, and separation of specimens in stages 1, 2 and 3 from specimens in stages 4 and 5 to form two broad clusters in both (Fig. 5C and 5D).

Unlike the above-mentioned stricter and significant separations of TSL, MB and FAL, less stricter values were observed which formed two separate and broad clusters where TSL and FAL were below 39 mm and 89 mm, respectively, for specimens in stages 1, 2 and 3. Exceptions to this pattern were observed as six stage 1, 2 and 3 specimens had TSL ≥ 39 mm and FAL ≥ 89 mm (TM47993, TM48000, TM48008, TM48052, TM48165 and TM48219). In addition, three stage 4 specimens (TM48002, TM48083 and TM48223) and one stage 5 individual (TM48229) formed part of the smaller sized group. Meanwhile, specimens in stages 4 and 5, had TSL ≥ 39 mm and FAL ≥ 89 mm except for the four

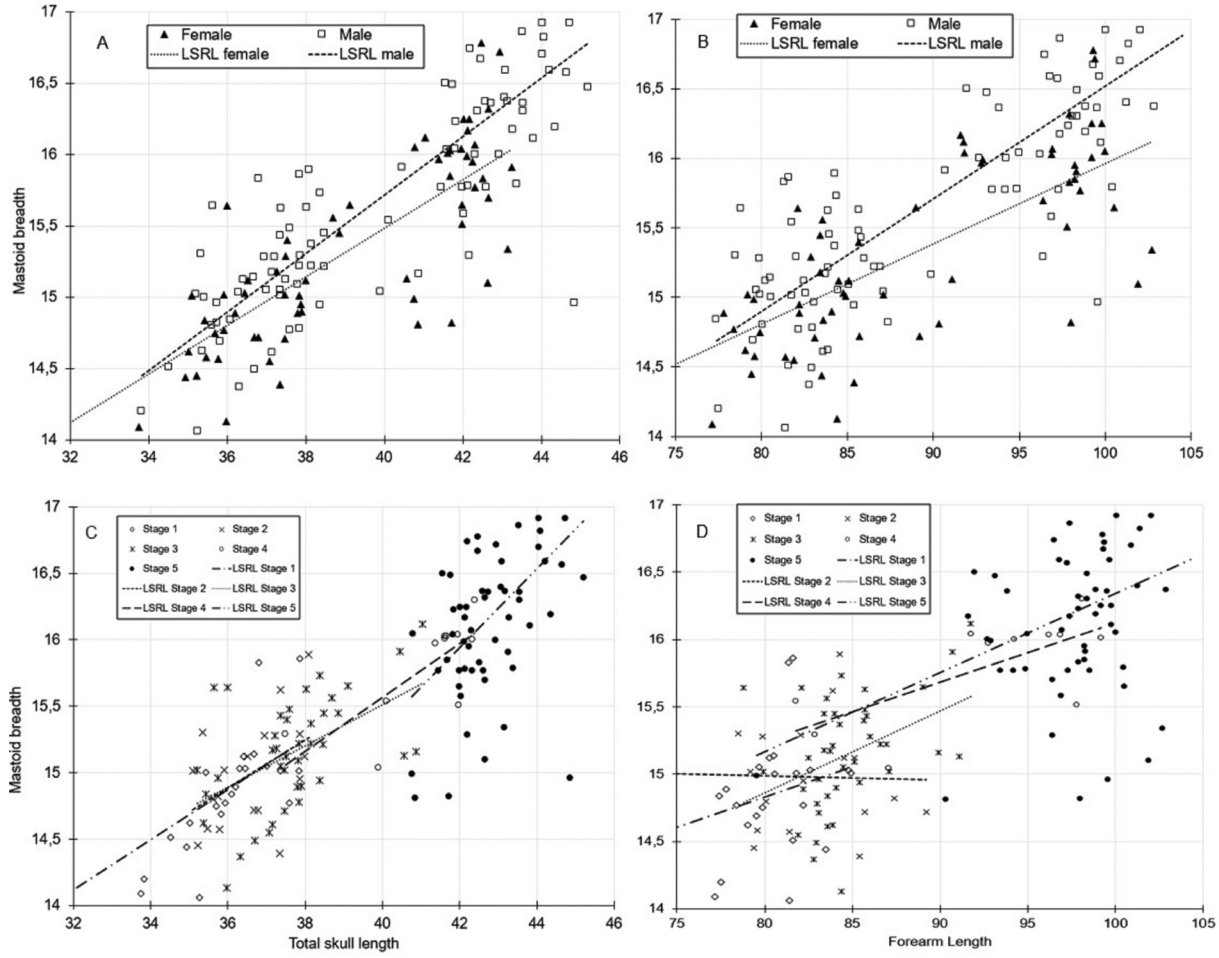

FIG. 5. Scatter plots depicting female (opaque triangle) and male (empty square) measurements for (A) total skull length versus mastoid breadth, and (B) forearm length versus mastoid breadth. The scatter plots for growth development stages 1–5 are depicted for (C) total skull length versus mastoid breadth, and (D) forearm length versus mastoid breadth. Linear size trends across different sexes and stage groups are shown by least squares regression lines (LSRL) for each tile

smaller stage 4 and 5 specimens mentioned above (Fig. 5). Of the exceptions, three specimens had a combination of TSL ≥ 39 mm and FAL < 90 mm (TM47993, TM48223 and TM48229). Two stage 4 specimens have the combination lower TSL < 39 mm and FAL < 90 mm (TM48002 and TM48083), whilst three stage 3 specimens have the combination TSL ≥ 39 mm and FAL ≥ 90 mm (TM48000, TM48008 and TM48052).

The mean and SD limits of the aforementioned specimens which do not cluster with their respective group stages are explained. The TSL for the stage 3 males, TM47993 (TSL = 40.88 mm) and TM48052 (TSL = 40.46 mm) is > 1SD above the SD limit (Table 3) whilst the MB of TM48052 is > 2SDs above the SD limit. These two specimens caused the high maximums that overlap with the stage 4 and 5 minimums (Fig. 4). In addition, the TSL, MB and FAL of the two stage 3 females, TM48000 and TM48008, caused the maximums to overlap with the larger sized groups. In contrast, three stage 4 specimens, one female (TM48083) and two males (TM48002 and TM48223), are clustered together with the smaller stage 3 specimens on PC1. The female TM48083, despite having all the cranial bone fusion characters of the stage 4 group, has a relatively smaller DENL (29.23 mm), FAL (82.9 mm) and TSL (37.49 mm) which are all more than two SDs below the mean for the stage 4 group (Fig. 4 and Table 3). Similarly, two females (TM48233, TM48229) of the larger sized stage 5 scored lower on PC1 and placed closer to stages 1–3 (Fig. 3). The MB, TSL and FAL of these two specimens were less than one1 SD below the lower SD limit for stage 5 females (Table 3). This has caused the stage 5 minimums of the MB, TSL and FAL to overlap with the smaller sized groups.

A linear DFA was performed to test the predictability of assigning specimens to growth development stages that are based on observed suture and

TABLE 3. The mean, standard deviation (SD), maximum (max.) and minimum (min.) of growth stages 1–5 for the measured variables (mm). Sample sizes for all (n = 153), female (n = 62), and male (n = 91) is shown. Abbreviations: MB — mastoid breadth, TSL — total skull length, FAL — forearm length, RW — rostral width, RL — rostral length, DENL — dental length, BW — braincase width

Variables		1			2			3			4			5		
		All	♀	♂	All	♀	♂	All	♀	♂	All	♀	♂	All	♀	♂
MB	$\bar{x}$	14.84	14.68	14.94	14.98	14.79	15.29	15.15	15.14	15.16	15.80	15.81	15.78	16.21	15.82	16.41
	SD	0.45	0.30	0.51	0.40	0.27	0.39	0.43	0.51	0.39	0.39	0.32	0.50	0.61	0.55	0.55
	max.	15.86	15.03	15.86	15.89	15.12	15.89	16.12	16.12	15.91	16.30	16.04	16.30	17.35	16.78	17.35
	min.	14.06	14.09	14.06	14.39	14.39	14.80	14.13	14.13	14.37	15.04	15.29	15.04	14.81	14.81	14.96
TSL	$\bar{x}$	35.81	35.20	36.21	36.54	36.42	36.71	37.68	37.87	37.57	41.13	41.01	41.26	42.90	42.15	43.29
	SD	1.55	1.93	1.16	1.04	1.02	1.14	1.43	1.58	1.35	1.45	1.74	1.19	1.10	0.70	1.08
	max.	37.85	37.83	37.85	38.09	37.99	38.09	41.04	41.04	40.88	42.38	41.97	42.38	45.20	43.25	45.20
	min.	31.03	31.03	33.83	35.09	35.09	35.34	35.21	35.43	35.21	37.49	37.49	39.90	40.75	40.75	41.45
FAL	$\bar{x}$	80.16	79.52	80.57	82.35	82.38	82.30	84.74	85.09	84.53	92.63	93.57	91.50	97.76	97.03	98.14
	SD	3.07	4.59	1.60	3.65	4.10	3.11	2.78	3.20	2.54	6.14	5.97	6.84	3.89	5.03	3.14
	max.	84.90	84.90	82.60	89.20	89.20	87.40	91.75	91.75	90.70	99.20	99.20	98.10	104.50	102.70	104.50
	min.	70.25	70.25	77.40	74.50	74.50	78.50	78.80	81.90	78.80	81.80	82.90	81.80	79.55	79.55	91.95
RW	$\bar{x}$	8.89	8.87	8.91	9.04	9.05	9.02	9.24	9.25	9.24	9.97	9.86	10.10	10.55	10.31	10.67
	SD	0.46	0.51	0.44	0.27	0.31	0.21	0.49	0.57	0.44	0.74	0.88	0.59	0.50	0.59	0.40
	max.	9.57	9.57	9.52	9.51	9.51	9.29	10.41	10.13	10.41	11.17	11.17	10.85	11.58	11.34	11.58
	min.	7.87	7.87	8.11	8.59	8.59	8.72	8.23	8.23	8.41	8.78	8.78	9.47	8.85	8.85	9.75
RL	$\bar{x}$	12.10	11.90	12.23	12.31	12.27	12.37	12.90	12.94	12.88	14.23	14.17	14.30	14.91	14.65	15.04
	SD	0.67	0.81	0.58	0.50	0.44	0.62	0.60	0.61	0.61	0.78	1.00	0.48	0.64	0.55	0.65
	max.	13.37	13.37	13.12	13.04	12.90	13.04	14.32	14.14	14.32	15.33	15.33	14.82	16.49	15.83	16.49
	min.	10.43	10.43	11.05	11.21	11.21	11.44	11.63	12.02	11.63	12.33	12.33	13.64	13.58	13.58	13.62
DENL	$\bar{x}$	27.90	27.48	28.16	28.63	28.71	28.50	29.43	29.61	29.32	32.02	32.58	31.35	34.07	33.46	34.39
	SD	1.17	1.62	0.73	1.20	1.32	1.07	1.31	1.34	1.31	2.13	1.73	2.56	1.10	0.79	1.12
	max.	29.74	29.74	29.02	31.37	31.37	29.95	32.42	32.42	32.33	34.43	34.30	34.43	36.74	35.09	36.74
	min.	24.02	24.02	26.86	26.59	26.59	26.88	26.92	27.73	26.92	28.45	29.23	28.45	31.97	31.97	32.53
BW	$\bar{x}$	16.09	15.96	16.18	16.08	15.98	16.23	16.37	16.39	16.36	17.17	17.11	17.24	17.58	17.33	17.72
	SD	0.48	0.46	0.49	0.39	0.32	0.46	0.44	0.43	0.46	0.57	0.50	0.70	0.50	0.55	0.42
	max.	16.87	16.68	16.87	16.64	16.52	16.64	17.27	17.27	17.02	18.12	17.71	18.12	18.56	17.99	18.56
	min.	15.07	15.13	15.07	15.39	15.39	15.51	15.06	15.53	15.06	16.22	16.47	16.22	15.95	15.95	16.98

dental groupings relative to assigned groupings in linear morphometric size. Equal variances were found for PC1 and PC2 (Levene's test, centered on the mean). The overall prediction accuracy was 69% for the combined data set (n = 153) and improved from younger to older specimens in the combined (stage 1 = 65%, stage 3 = 75% and stage 5=97%), females (stage 1 = 67%, stage 3 = 67% and stage 5 = 90%) and males (stage 1 = 50%, stage 3 = 76% and stage 5 = 100%). (Table 4). Meanwhile, poor predictions were obtained for combined sexes of stages 2 and 4 which both had zero correct predictions (Table 4). Predictions for females (n = 62) of stages 1, 3, and 5 were correct for 6/9, 10/15 and 19/21 specimens, respectively (Table 4). Again, predictions were poor for the stages 2 and 4. For males (n = 91), predictions were highest for stage 3 (19/25) and stage 5 (40/40). Stage 1 had an accuracy of 50% (7/14), with six specimens assigned to stage 3. Stages 2 and 4 specimens had zero correct predictions (Table 4).

DISCUSSION

Of the five *R. aegyptiacus* (n = 153) cranial bone fusion and dental based growth development stages assessed, evidence from the present study showed that three (stages 1, 3 and 5) can be predicted in linear morphometrics with over 65% accuracy. Prediction for stages 2 and 4 was unreliable (0%) owing to the high overlap with preceding and successive stages. Grouping specimens into growth stages using cranial bone fusion is based on the logic that the progression of cranial suture closure and eventual fusion is associated with skull growth and age (Opperman, 2000; Monrroy *et al.*, 2019). When all five stages were aligned to linear measurements, a significant size difference was found between specimens assigned to stages 1, 2 and 3 of TSL < 36 mm, MB < 14.8 mm and FAL < 85 mm, which had fewer fused cranial sutures, compared to the larger sized specimens in stages 4 and 5 of TSL > 42 mm, MB > 16 mm and FAL > 97 mm, which had more

fused cranial sutures. The inference can therefore be made that the smaller specimens in stages 1, 2 and 3 can be qualitatively regarded as younger compared to the larger, and older specimens in stages 4 and 5.

Comparing our quantitative assessment of suture fusion with assessments in *Pteropus* sp. (Giannini *et al.*, 2006) and *N. leporinus* (Monrroy *et al.*, 2019) showed differences and consistencies. The stages 1, 2 and 3, albeit differing by level of tooth eruption, was either completely or partially unfused for the basicranial (sspo), occipital (spip, sopa and soipa) and vault (sc and ss) regions of the skull. However, Giannini *et al.* (2006) found completely unfused basicranial (sspo) and occipital (sopa) sutures in their stages 1–3 of *Pteropus* sp. whilst Monrroy *et al.* (2019) only observed early fusion of the sspo and sopa sutures from a fifth stage of development, reported as a late juvenile stage E, in their assessment of *N. leporinus*.

Specimens categorized as stage 4 in the present study had fused sutures of the basicranial (sspo) and occipital (sopa) regions, whilst early development of the sagittal ridge (cs) was observed at stages 3 and 4. Similarly, Giannini *et al.* (2006) observed fused sutures of the basicranial (sspo) and occipital (sopa) regions at their stage 4 for *Pteropus* sp. whilst, in *N. leporinus*, Monrroy *et al.* (2019) recorded partial degrees of suture fusion of only 40% and 20%, respectively, for sspo and sopa in their stage F, regarded as a subadult stage. Consistent with the stage 4 specimens of the present study, the coronalis was unfused in Giannini's *et al.* (2006) stage 4, whilst Monrroy *et al.* (2019) recorded partial degrees of fusion of 15% and 40% at stages E (late juvenile) and F (subadult), respectively. At stage 5, we observed fused sutures of the basicranial, occipital and vault regions. Giannini *et al.* (2006) observed fused sagittalis and occipital sutures (spip and soipa) earlier at stage 2. Monrroy *et al.* (2019) found the sutures ss, spip and soipa fused at their stage F and G (adult stage) although some degree of fusion was observed stage E (spip = 25%, soipa = 50%) and stage F (ss = 15%). From a qualitative perspective, the development from young to old specimens in *R. aegyptiacus* based on characteristics associated with age (cranial bone fusion and tooth eruption) can be expressed in growth stages, as indicated by Giannini *et al.* (2006) and Monrroy *et al.* (2019).

Previous age prediction studies that were based on linear morphometric size focused on young juveniles of less than a year old (Stern and Kunz, 1998; Baptista *et al.*, 2000; Cheng and Lee, 2002; Elangovan *et al.*, 2002, 2003; Chaverri and Kunz, 2006; Allen *et al.*, 2010; Jin *et al.*, 2010; Chaverri and Vonhof, 2011; Chen *et al.*, 2016; Eghbali and Sharifi, 2018). These studies further recorded the date at birth and calculated growth rates using rapid early development of forearm length and epiphyseal gap as variables. The results of these authors all agree that these variables became less reliable with

TABLE 4. Prediction matrix of stages 1–5 for the combined female and male data sets of *R. aegyptiacus* calculated using linear discriminant function analysis. The accuracy percentage of each test and stage is shown in parenthesis. PC1 and PC2 scores both showed equal variances and were included for the analysis. Observed and calculated outliers are included in the analysis

Actual stages	Predicted stages					*n*
	Stage 1	Stage 2	Stage 3	Stage 4	Stage 5	
Stage 1	15* (65%)	0	8	0	0	23
Stage 2	6	0	12	0	0	18
Stage 3	5	0	31** (75%)	2	2	40
Stage 4	0	0	3	0	8	11
Stage 5	0	0	2	0	59*** (97%)	61
			♀♀ *n* = 62 (61%)			
Stage 1	6* (67%)	1	2	0	0	9
Stage 2	3	3	5	0	0	11
Stage 3	0	3	10* (67%)	0	2	15
Stage 4	0	0	1	0	5	6
Stage 5	0	0	2	0	19*** (90%)	21
			♂♂ *n* = 91 (73%)			
Stage 1	7	1	6	0	0	14
Stage 2	2	0	5	0	0	7
Stage 3	4	0	19** (76%)	2	0	25
Stage 4	0	0	2	0	3	5
Stage 5	0	0	0	0	40*** (100%)	40

*** > 95% accuracy; ** 75% accuracy; * > 65% accuracy

advancing age as epiphyseal gap fused completely by three months, whilst forearm length grew at a substantially slower rate in older bats. Unlike the aforementioned studies which referred to chronological age, we focused on bats of unknown birth date and age which limited our findings to the more relative biological estimate of age (Brunet-Rossinni and Wilkinson, 2009).

In terms of interpreting the five established growth development stages in linear morphometrics for both sexes, notwithstanding prediction accuracy, it is difficult to predict a specific stage to a fixed set of linear measurements due to the spread and overlap amongst the different stages, especially stages 2 and 4. A reliable and significant separation, with no overlap, of the smallest specimens in stages 1, 2 and 3 from the largest specimens in stages 4 and 5 was made using TSL. Albeit significant, separations using MB and FAL were less reliable due to some overlap. This could be attributed to intraspecific anatomical and morphological variations in the growth pattern of the species which can arise from microenvironmental and dietary differences at time of birth and development (Brunet-Rossinni and Wilkinson, 2009).

Despite specimens from the present study being caught at different times of the year (see Swanepoel *et al.*, 2007), no significant differences were found between the growth pattern and separation from each period. Nonetheless, we obtained significant values in cranial and forearm linear size which separated *R. aegyptiacus* into younger, consisting of stages 1, 2 and 3, and older, consisting of stages 4 and 5, specimens. This separation was only identified in TSL whilst overlap between groups was observed for MB and FAL.

Morphometrics studies on older bats have predominantly focused on distinguishing species and sex by identifying intraspecific (sexual dimorphism) and interspecific size thresholds (Storz *et al.*, 2001; Taylor and Monadjem, 2008; Jarrín-V. *et al.*, 2010; Welbergen, 2010; Shahbaz *et al.*, 2014). The present study did not find significant sexual dimorphism across most *R. aegyptiacus* specimens except for two stage 5 females. Males were, however, observed to be relatively larger than females with increasing sizes of the measurements TSL, MB and FAL. Owing to relatively smaller RW and orbital foramens the two stage 5 females were suspected to be different species, although field and post sequence (16SrRNA) identification by the original collectors (Swanepoel *et al.*, 2007) identified them as *R. aegyptiacus*.

In summary, the present study shows evidence of age prediction through linear morphometrics for *R. aegyptiacus* which can be expressed into two distinct groups of young and old cohorts. Accurate morphometric predictions of age have been made in longitudinal studies (temporal, mark-recapture), through equations that rely on the rapidly increasing morphological growth rate observed in younger bats of known birth date (Baptista *et al.*, 2000; Cheng and Lee, 2002; Elangovan *et al.*, 2002). For a cross sectional study that assessed specimens of unknown age (single time period, single capture), we relied on the examination of morphological characteristics (i.e., cranial suture, dental development and linear morphometric) which yield qualitative age-related categories (Baptista *et al.*, 2000; Cheng and Lee, 2002; Elangovan *et al.*, 2002; Brunet-Rossinni and Wilkinson, 2009). Quantitative age prediction methods that can be employed in specimens sampled from cross sectional studies include dental sectioning which relies on the annual growth of cementum layers on teeth that can be counted (Cool *et al.*, 1994; Divljan *et al.*, 2006). Examining the growth of cementum is, however, destructive as it requires the extraction of the targeted tooth unlike the rapid, non-invasive methods we employed. Nonetheless, inferences to chronological age can be made from morphological characteristics through comparison to cementum growth. This study therefore provides species specific baseline data for *R. aegyptiacus* cross sectional studies, which seek to predict age.

Supplementary Information

Contents: Supplementary Table S1. *Rousettus aegyptiacus* specimens used in this study from the Ditsong National Museum of Natural History. Specimens are sorted by sex. The age-related characteristics, tooth wear class and eruptions of second molar, are also noted for each specimen. Supplementary Information is available exclusively on BioOne.

Acknowledgements

This project was made possible through support from the South African Research Chair on Infectious Disease of Animals, of the Department of Science and Innovation, held by Professor Wanda Markotter (grant number 98339) administered by National Research Foundation. Specimens were provided by the Ditsong National Museum of Natural History small mammals collection. Further support was obtained from Defence Threat Reduction Agency and the National United Nations Children' Fund (UNICEF).

Author Contribution Statement

TTN: research concept and design, collection and/or assembly of data, data analysis and interpretation, writing the article,

critical revision and final approval of the article; TK and WM: Research concept and design, collection and/or assembly of data, data analysis and interpretation, critical revision and final approval of the article.

Literature Cited

Allen, L. C., C. S. Richardson, G. F. McCracken, and T. H. Kunz. 2010. Birth size and postnatal growth in cave- and bridge-roosting Brazilian free-tailed bats. Journal of Zoology (London), 280: 8–16. doi: 10.1111/j.1469-7998.2009.00636.x.

Baptista, T. L., C. S. Richardson, and T. K. Kunz. 2000. Postnatal growth and age estimation in free-ranging bats: a comparison of longitudinal and cross-sectional sampling methods. Journal of Mammalogy, 81: 709–718. doi: 10.1644/1545-1542(2000)081<0709:PGAAEI>2.3.CO;2.

Brunet-Rossinni, A. K., and S. N. Austad. 2004. Ageing studies on bats: a review. Biogerontology, 5: 211–222. doi: 10.1023/B:BGEN.0000038022.65024.d8.

Brunet-Rossinni, A. K., and G. S. Wilkinson. 2009. methods for age estimation and the study of senescence in bats. Pp. 315–325, *in* Ecological and behavioral methods for the study of bats, 2nd edition (T. H. Kunz and S. Parsons, eds.). Johns Hopkins University Press, Baltimore, xvii + 901 pp.

Chaverri, G., and T. H. Kunz. 2006. Reproductive biology and postnatal development in the tentmaking bat *Artibeus watsoni* (Chiroptera: Phyllostomidae). Journal of Zoology (London), 270: 650–656. doi: 10.1111/j.1469-7998.2006.00171.x.

Chaverri, G., and M. J. Vonhof. 2011. Reproduction and growth in a Neotropical insectivorous bat. Acta Chiropterologica, 13: 147–155. doi: 10.3161/150811011X578697.

Chen, S. F., S. S. Huang, D. J. Lu, and T. J. Shen. 2016. Postnatal growth and age estimation in *Scotophilus kuhlii*. Zoo Biology, 35: 35–41. doi: 10.1002/zoo.21251.

Cheng, H. C., and L. L. Lee. 2002. Postnatal growth, age estimation, and sexual maturity in the Formosan leaf-nosed bat (*Hipposideros terasensis*). Journal of Mammalogy, 83: 785–793. doi: 10.1644/1545-1542(2002)083<0785:PGAEAS>2.0.CO;2.

Cool, S. M., M. B. Bennet, and K. Romaniuk. 1994. Age estimation of pteropodid bats (Megachiroptera) from hard tissue parameters. Wildlife Research, 21: 353–364. doi: 10.1071/WR9940353.

Divljan, A., K. Parry-Jones, and G. M. Wardle. 2006. Age determination in the grey-headed flying fox. Journal of Wildlife Management, 70: 607–611. doi: 10.2193/0022-541X(2006)70[607:ADITGF]2.0.CO;2.

Eastick, D. L., S. R. Griffiths, J. D. L. Yen, and K. A. Robert. 2022. Size at birth, postnatal growth, and reproductive timing in an Australian microbat. Integrative Organismal Biology, 4: 1–13. doi: 10.1093/iob/obac030.

Eghbali, H., and M. Sharifi. 2018. Postnatal growth, age estimation, and wing development in Geoffroy's bat *Myotis emarginatus* (Chiroptera: Vespertilionidae). Mammal Study, 43: 153–165. doi: 10.3106/ms2017-0077.

Eghbali, H., S. Shahabi, N. Najafi, R. Mehdizadeh, S. Yousefi, and M. Sharifi. 2018. Postnatal growth, wing development and age estimations in the Mediterranean horseshoe bat *Rhinolophus euryale* (Chiroptera: Rhinolophidae) in Kerend cave, western Iran. Mammalia, 82: 276–287. doi: 10.1515/mammalia-2017-0006.

Elangovan, V., H. Raghuram, E. Yuvana Satya Priya, and G. Marimuthu. 2002. Postnatal growth, age estimation and development of foraging behaviour in the fulvous fruit bat *Rousettus leschenaulti*. Journal of Bioscience, 27: 695–702. doi: 10.1007/BF02708378.

Elangovan, V., E. Yuvana Satya Priya, H. Raghuram, and G. Marimuthu. 2003. Postnatal development in the Indian short-nosed fruit bat *Cynopterus sphinx*: growth rate and age estimation. Acta Chiropterologica, 5: 107–116. doi: 10.3161/001.005.0110.

Giannini, N. P., J. R. Wible, and N. B. Simmons. 2006. On the cranial osteology of Chiroptera. I. *Pteropus* (Megachiroptera: Pteropodidae). Bulletin of the American Museum of Natural History, 295: 1–134. doi: 10.1206/0003-0090(2006)295[0001:OTCOOC]2.0.CO;2.

Hayman, D. T. S. 2015. Biannual birth pulses allow filoviruses to persist in bat populations. Proceedings of the Royal Society, 282B: 20142591. doi: 10.1098/rspb.2014.2591.

Hayman, D. T. S., R. A. Bowen, P. M. Cryan, G. F. McCracken, T. J. O'Shea, A. J. Peel, A. Gilbert, C. T. Webb, and J. L. N. Wood. 2012*a*. Ecology of zoonotic infectious diseases in bats: current knowledge and future directions. Zoonoses Public Health, 60: 2–21. doi: 10.1111/zph.12000.

Hayman, D. T. S., R. McCrea, O. Restif, R. Suu-Ire, A. R. Fooks, J. L. N. Wood, A. A. Cunningham, and J. M. Rowcliffe. 2012*b*. Demography of straw-coloured fruit bats in Ghana. Journal of Mammalogy, 93: 1393–1404. doi: 10.1644/11-MAMM-A-270.1.

Hecht, L. 2021. The importance of considering age when quantifying wild animals' welfare. Biological Reviews, 96: 2602–2616. doi.org/10.1111/brv.12769.

Hielscher, R. C., J. A. Schultz, and T. Martin. 2015. Wear pattern of the molar dentition of an extant and an Oligocene bat assemblage with implications on functionality. Palaeobiodiversity and Palaeoenvironments, 95: 597–611. doi: 10.1007/s12549-015-0186-z.

Hood, W. R., J. Bloss, and T. H. Kunz. 2002. Intrinsic and extrinsic sources of variation in size at birth and rates of postnatal growth in the big brown bat *Eptesicus fuscus* (Chiroptera: Vespertilionidae). Journal of Zoology (London), 258: 355–363. doi: 10.1017/S0952836902001504.

Hyatt, A. D., P. Daszak, A. A. Cunningham, H. Field, and A. R. Gould. 2004. Henipaviruses: gaps in the knowledge of emergence. EcoHealth, 1: 25–38. doi: 10.1007/s10393-004-0017-6.

Jarrín-V., P., C. Flores, and J. Salcedo. 2010. Morphological variation in the short-tailed fruit bat (*Carollia*) in Ecuador, with comments on the practical and philosophical aspects of boundaries among species. Integrative Zoology, 5: 226–240. doi: 10.1111/j.1749-4877.2010.00208.x.

Jin, L., A. Lin, K. Sun, Y. Liu, and J. Feng. 2010. Postnatal growth and age estimation in the ashy leaf-nosed bat, *Hipposideros cineraceus*. Acta Chiropterologica, 12: 155–160. doi: 10.3161/150811010X504653.

Keeling, M. J., and P. Rohani. 2008. Modelling infectious diseases in humans and animals. Princeton University Press, Princeton, N.J., 384 pp. doi: 10.2307/j.ctvcm4gk0.

Lloyd-Smith, J. O., P. C. Cross, C. J. Briggs, M. Daugherty, W. M. Getz, J. Latto, M. S. Sanchez, A. B. Smith, and A. Swei. 2005. Should we expect population thresholds for wildlife disease? Trends in Ecology and Evolution, 20: 511–519. doi: 10.1016/j.tree.2005.07.004.

Markotter, W., J. Coertse, L. De Vries, M. Geldenhuys, and

M. Mortlock. 2020. Bat-borne viruses in Africa: a critical review. Journal of Zoology (London), 311: 77–98. doi: 10.1111/jzo.12769.

Monadjem, A., P. J. Taylor, F. P. D. Cotterill, and M. C. Schoeman. 2020. Bats of southern and central Africa: a biogeographic and taxonomic synthesis. Wits University Press, Johannesburg, 730 pp.

Monrroy, G. A., N. Reyes-Amaya, and A. Jerez. 2019. Postnatal cranial ontogeny of the greater bulldog bat *Noctilio leporinus* (Chiroptera: Noctilionidae). Acta Zoologica, 101: 412–430. doi: 10.1111/azo.12309.

Noll, U. G. 1979. Postnatal growth and development of thermogenesis in *Rousettus aegyptiacus*. Comparative Biochemistry and Physiology, 63A: 89–93. doi: 10.1016/0300-9629(79)90632-7.

Oli, M. K., and T. Coulson. 2016. Life history, what is? Pp. 394–399, *in* Encyclopedia of evolutionary biology. Volume 2 (R. M. Kliman, ed.). Academic Press, Oxford, 2132 pp. doi: 10.1016/B978-0-12-800049-6.00083-4.

Opperman, L. A. 2000. Cranial sutures as intramembranous bone growth sites. Developmental Dynamics, 219: 472–485. doi: 10.1002/1097-0177(2000)9999:9999<::AID-DVDY1073>3.0.CO;2-F.

Pawęska, J. T., P. Jansen van Vuren, A. Kemp, N. Storm, A. A. Grobbelaar, M. R. Wiley, G. Palacios, and W. Markotter. 2018. Marburg virus infection in Egyptian rousette bats, South Africa, 2013–2014. Emerging Infectious Diseases, 24: 1134–1137. doi: 10.3201/eid2406.172165.

R Core Team. 2021. R: a language and environment for statistical computing. R Foundation for Statistical Computing, Vienna, Austria. Available at https://www.R-project.org.

Schmieder, D. A., H. A. Benítez, I. M. Borissov, and C. Fruciano. 2015. Bat species comparisons based on external morphology: a test of traditional versus geometric morphometric approaches. PLoS ONE, 10: e0127043. doi: 10.1371/journal.pone.0127043.

Schwertman, N. C., M. A. Owens, and R. Adnan. 2004. A simple more general boxplot method for identifying outliers. Computational Statistics & Data Analysis, 47: 165–174. doi:10.1016/j.csda.2003.10.012.

Shahbaz, M., A. Javid, T. Javed, M. Mahmood-Ul-Hassan, and S. M. Hussain. 2014. Morphometrics of fulvous fruit bat (*Rousettus leschenaulti*) from Lahore, Pakistan. Journal of Animal & Plant Sciences, 24: 955–960.

Son, N. T., M. Motokawa, T. Oshida, V. D. Thong, G. Csorba, and H. Endo. 2015. Multivariate analysis of the skull size and shape in tube-nosed bats of the genus *Murina* (Chiroptera: Vespertilionidae) from Vietnam. Mammal Study, 40: 79–94. doi: 10.3106/041.040.0203.

Stern, A. A., and T. H. Kunz. 1998. Intraspecific variation in postnatal growth in the greater spear-nosed bat. Journal of Mammalogy, 79: 755–763. doi: 10.2307/1383086.

Storz, J. F., J. Balasingh, H. R. Bhat, P. T. Nathan, D. P. S. Doss, A. A. Prakash, and T. H. Kunz. 2001. Clinal variation in body size and sexual dimorphism in an Indian fruit bat, *Cynopterus sphinx* (Chiroptera: Pteropodidae). Biological Journal of the Linnean Society, 72: 17–31. doi: 10.1111/j.1095-8312.2001.tb01298.x.

Swanepoel, R., S. B. Smit, P. E. Rollin, P. Formenty, P. A. Leman, A. Kemp, F. J. Burt, A. A. Grobbelaar, J. Croft, D. G. Bausch, *et al*. 2007. Studies of reservoir hosts for Marburg virus. Emerging Infectious Diseases, 13: 1847–1851. doi: 10.3201/eid1312.071115.

Taylor, P. J., and A. Monadjem. 2008. Maxillary shape as a diagnostic tool for identifying fruit bats, *Epomophorus crypturus* and *E. wahlbergi* from museum specimens and in the field. South African Journal of Wildlife Research, 38: 22–27. doi: 10.3957/0379-4369-38.1.22. doi: 10.3957/0379-4369-38.1.22.

Welbergen, J. A. 2010. Growth, bimaturation, and sexual size dimorphism in wild gray-headed flying foxes (*Pteropus poliocephalus*). Journal of Mammalogy, 91: 38–47. doi: 10.1644/09-MAMM-A-157R.1.

Wilkinson, G. S. and J. M. South. 2002. Life history, ecology and longevity in bats. Aging Cell, 1: 124–131. doi: 10.1046/j.1474-9728.2002.00020.x.

Received 14 March 2023, accepted 25 May 2023

Associate Editor: Wiesław Bogdanowicz